2021 © The Japan Society for Analytical Chemistry

Internet of Things Implementation of Nitrate and Ammonium Sensors for Online Water Monitoring

Ismail AGIR,*† Ridvan YILDIRIM, Mustafa NIGDE,** and Ibrahim ISILDAK****

**Department of Bioengineering, Faculty of Engineering and Natural Sciences, Istanbul Medeniyet University, Uskudar, Istanbul, 34720, Turkey*
***Department of Bioengineering, Faculty of Chemical and Metallurgical Engineering, Yildiz Technical University, Esenler, Istanbul, 34220, Turkey*

In this work, we proposed a new wireless sensor to contribute to research aimed at continuous monitoring of nitrate and ammonium in water, which as leading agents of water pollution have become the source of a serious problem today. In this research, a well-implemented application of an electroanalytical sensor was achieved by combining it with the internet of things (IoT) concept, which is the most modern technique for wireless data collection. We developed a portable IoT system and ion-selective nitrate and ammonium electrodes and monitored the nitrate and ammonium levels of the water online. The system was produced in a low-cost manner (under $25) and it enabled data acquisition without energy-related problems, thanks to the support of solar energy and mobile power bank. The recovery rates of the sensors were tested with the standard addition method and response was obtained between 101.74 and 147.01%.

Keywords Water quality monitoring, ion-selective electrode, internet of things

(Received October 30, 2020; Accepted November 21, 2020; Advance Publication Released Online by J-STAGE November 27, 2020)

Introduction

As a result of the widespread use of the internet and ongoing advancement of technology, devices used in our daily lives are now constantly connected to the internet. The universal set of devices and data networks that can connect to the internet is called the internet of things.[1] Thanks to the great advances made in data science, nanotechnology, and measurement techniques in recent years, innovations have also emerged in sensor technologies. These innovations have enabled us to develop new sensor applications such as smart sensors, IoT sensors, and multi-sensors in various fields, although the nomenclature or definitions differ in the literature.[2-7]

Water pollution is one of the leading problems that needs to be solved to protect human life and the environment.[8] To protect human and environmental health, continuous monitoring and analysis of harmful contaminant levels in freshwater resources are mandatory. Therefore, more attention has been given to the development of sensors that can analyze water quality in recent years.[9]

Nitrogen is an indispensable nutrient for the ecosystem and plant life.[10] Environmentally important nitrogen compounds including ammonium (NH_4^+), nitrate (NO_3^-), and nitrite (NO_2^-) are formed within the nitrogen cycle and affects all forms of life *via* direct and indirect routes.[11] Nitrate and ammonium are leading water pollutants in ground and surface water systems. Nitrate is spread particularly, but not exclusively, by unconstrained agricultural use of synthetic fertilizers, and poses a real threat to human health[12,13] but the presence of ammonium in drinking water is not as serious.[14] However, ammonium can be converted to nitrite and an abundance of it may cause excessive nitrification in water bodies, which is another issue for environmental well-being.[15] Because these issues cannot be ignored, continuous monitoring of affected water bodies is required to maintain the water quality within acceptable levels.[12] Even though measuring the levels of ammonium and nitrate ions *via* several well-established methods, such as UV-Vis spectrophotometry or colorimetry,[16] can provide valuable information, all of these methods have some difficulties such as needing laboratory conditions, frequent sampling, and transportation of samples. A well-implemented wireless sensing system involving nitrate and ammonium sensors can help mitigate such problems by continuous acquisition and transfer of necessary water quality data.[17-19]

There are many studies in the literature on new measurement techniques for ammonium and nitrate in water. In one study, an electronic tongue system was established for on-site and continuous measurement,[20] and in another study nitrate and ammonium were measured simultaneously.[12] However, these studies did not enable online monitoring due to the lack of a wireless network connection. One study reported the development of a multiple ion meter system,[21] and another reported the development of a computer dependent online ion measurement system,[22] but these studies did not take advantage of wireless sensor network (WSN) technology as well. Monitoring of ammonium and nitrate with WSN was reported in another paper, but the network structure used was GSM-based and not Wi-Fi.[23] There have also been WSN-based nitrate-only measurement studies using microelectronics and energy harvesting.[24,25]

† To whom correspondence should be addressed.
E-mail: agr.isml@gmail.com

Table 1 Compositions of the ammonium and nitrate cocktails (w/w %)

	PVC	KTpCIPB	Plasticizer	Ionophore
NO_3^- ISE	28	—	68 (DBP)	4 (TDDAN)
NH_4^+ ISE	32	0.5	66 (BEHS)	1.5 (Nonactin)

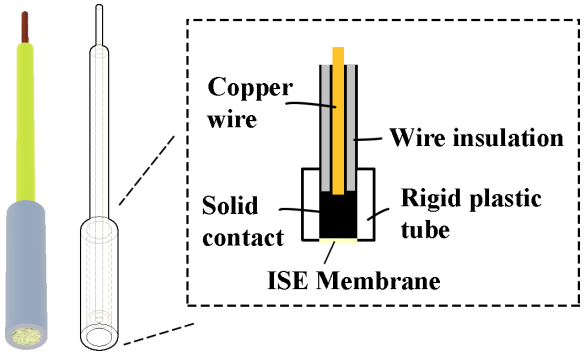


Fig. 1 Conceptual drawing of the ISE.

In our study, the levels of both free nitrate and ammonium ions in water were simultaneously monitored online with an IoT system that is portable, low in cost, accessible from the World Wide Web, and capable of any multi ion-selective electrode sensor measurement with smart features such as calibration and control.

Experimental

Reagents and chemicals

Tetrahydrofuran (THF) and high molecular weight poly(vinyl chloride) (PVC), potassium tetrakis(4-chlorophenyl)borate (KTpCIPB), ammonium ionophore I (nonactin), bis(2-ethylhexyl) sebacate (BEHS), and dibutyl phthalate (DBP) tetradodecylammonium nitrate (TDDAN) were purchased from Sigma-Aldrich and used without further purification in the preparation of the membranes. Graphite (Sigma-Aldrich, USA), epoxy (Macroplast Su 2227, Henkel, Germany), and hardener (Desmodur RFE, Bayer AG, Germany) were used in the preparation of the solid contact material. All cationic and anionic standard solutions were prepared using analytical grade nitrate or chloride salts, sodium, or potassium salts, respectively. Ultrapure water (18.2 MΩ cm^{-1}) was obtained *via* an ultrapure system Purelab Flex 4 (ELGA LabWater, UK). All ISE potentials were measured against the silver/silver chloride reference electrode, which was elaborated in our laboratory.

Preparation of membrane cocktails and ISEs

As in our previous work,[26] we prepared solid-contact paste after dissolving 50% graphite oxide, 35% epoxy, and 15% hardener in a few drops of THF. Then, the paste was filled into polypropylene tubes (2.5 mm inner diameter, 3.5 mm outer diameter, 50.0 mm length) and attached to a copper wire from one end for establishing a signal connection. The filled tubes were left to dry in a dark, cool closet overnight. Membrane cocktails were prepared by dissolving the chemicals listed in Table 1 in 3 mL THF. As shown in Fig. 1, the all-solid-state ISEs were prepared according to steps similar to that described in our previous work.[27] Next, solid-contact filled tubes were dipped in membrane cocktails several times to obtain a thin layer of membrane on the surface. Coated electrodes were first left to dry, then conditioned in 10^{-2} mol L^{-1} standard solution of the related ion overnight.

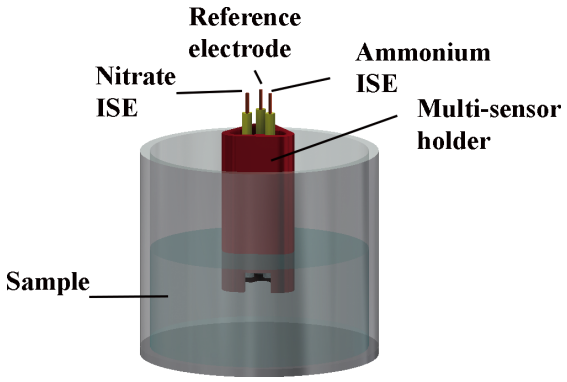


Fig. 2 Conceptual measurement cell.

Potentiometric measurements of the electrodes were taken in a cell assembly: double junction Ag/AgCl RE ‖ sample solution | PVC membrane | solid-contact | copper wire. Potentiometric cell is shown in Fig. 2.

Low cost IoT sensor system

The IoT-based smart sensor system circuit was designed and assembled on a printed circuit board (FR-2, PCB), as shown in the diagram in Fig. 3. This system can acquire multiple ion-selective electrode signals *versus* a reference electrode. A lithium-ion battery based mobile power bank can be charged by any energy harvesting system, such as a photovoltaic (PV) panel. We used a 12 V, 20 W solar panel. With two step-down modules, LM2596 by Texas Instruments (TI, USA), we regulated the PV output voltage to 5 V for charging and the power bank output to 3.3 V to run the system.

Due to the high impedance of the ion-selective electrodes,[28] the signal must be buffered with the op-amp. A single op-amp (LMP7721, TI, USA) was used in the system for multiple ion-selective electrode input, thus reducing total cost. We selected LMP7721 because it is very suitable for our high impedance sensor application due to its low voltage noise (6.5 nV/$\sqrt{\text{Hz}}$) and low input bias current (3 femtoampere).[29] The signal path that is established with a single op-amp can be multiplied with an analog multiplexer integrated circuit (IC) up to 16, which has the least impact on the signal (CD74HC4067, TI, USA). The system, under the control of a microcontroller (MCU) Arduino Pro Mini (Arduino AG), reads all sensors one by one in a time sequence with 10 ms delay, then sends all data at one time in 15 s intervals. Since the system receives its energy from a battery through a mobile power bank, it is a single-ended circuit and hence it has no negative voltage source. When ISEs output a negative voltage as a signal, a bias voltage must be added to the reference voltage so that the analog-digital converter (ADC) can quantize it. This addition was made using high precision, low noise 1024 mV voltage reference (LM4140-ACM, TI, USA) to the reference electrode using another op-amp (LMP7715, TI, USA). Finally, a resistor voltage divider made with two 10 kΩ resistor (ERJT06, Panasonic Corp., Japan) was added to the signal path to reduce this bias to 512 mV.

Analog input of the MCU was used to read the potential signals. The 3.3 V 8 MHz version of the Arduino Pro Mini used

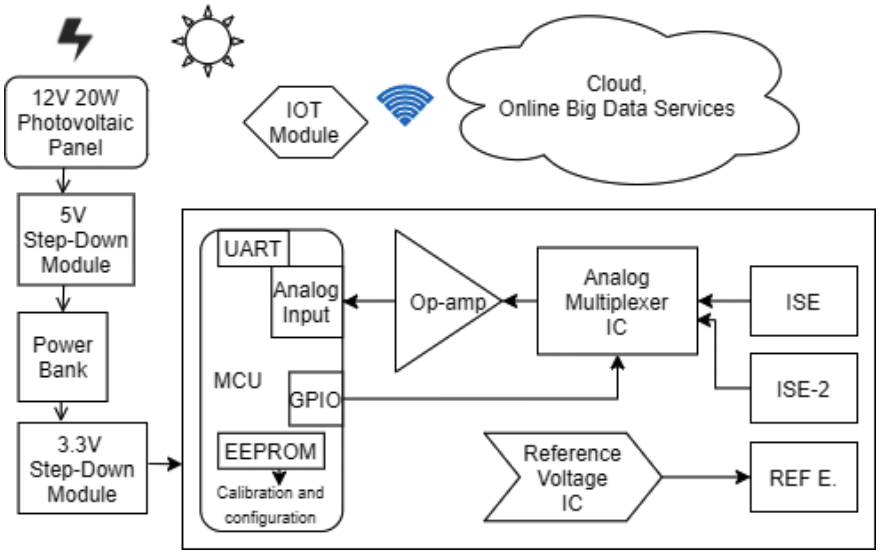


Fig. 3 Block diagram of the IoT sensor data acquisition system.

contains 10-bit resolution ADC. By setting the microcontroller to enable the 1.1 V internal reference for ADC, the full-scale input range is 1.1 V, then the smallest readable voltage step (LSB) can be calculated as 1.07 mV according to Eq. (1):[30]

$$\text{LSB} = (\text{Full scale voltage})/(2\text{^resolution bits}) \quad (1)$$

Also, we applied a software-based moving average filter to the ADC results for noise reduction. Theoretically, considering that the sensors follow the Nernst equation and taking an operating range of 10^{-1} to 10^{-5} mol L^{-1}, a signal of approximately ±235 mV is expected, so the midpoint of 512 mV turns out to be suitable and therefore the op-amp was set in the unity-gain configuration.

Using EEPROM in the MCU, it is ensured that the information such as operational parameters, calibration data, Wi-Fi password, and cloud connection keys were recorded. The MCU was connected to the Wi-Fi network using a low-cost IoT module (ESP-12F, Ai-Thinker Co., PRC) attached to the serial port (UART). Thanks to the IoT module, the converted sensor signal was transferred to cloud servers (ThingSpeak.com, MathWorks, USA) with the HTTP GET method.

Multi sensor head and enclosure

To be able to use nitrate and ammonium sensors at the same time, we fabricated a 3D printed multi-sensor holder (Fig. 2) using polylactic acid (PLA) filament (UZARAS 3D, Turkey). The holder was designed to be interchangeable with the sensors, to provide the necessary mechanical support while taking measurements from the water, and to make robust electronic connections. A plastic box housing the IoT system was designed and assembled in the same way and for the same purposes as the holder.

IoT application

Sensors were connected to the PCB with crocodile cable. An external antenna with 3 dBi gain was installed in the IoT module. A Wi-Fi connection was established with an internet access point (router, DSL-AC51, ASUSTeK Computer Inc., Taiwan). As shown in Fig. 4 (captured from https://atlas.harita.gov.tr/, HGM Atlas, Turkey), the distance of the sensors to the access point was set at approximately 30 meters. The IoT system was set up and operated to receive two sensor measurements per 15 s. After calibration was done, we switched the IoT module to web server mode and instructed calibration data to the device's memory. Then the system started to post both raw and calibrated sensor data to the internet simultaneously. All data was stored in our ThingSpeak (MathWorks, USA) cloud account and then was downloaded and analyzed with the Python programming language.



Fig. 4 Map showing the distance between access point and the IoT system.

Results and Discussion

To measure both nitrate and ammonium in water simultaneously with ion-selective electrodes, an IoT system with a total cost of less than $25 was implemented by providing dedicated component selection and circuit design. The IoT system was run wirelessly without a problem. Sensor measurement data was successfully transferred to a cloud server, which means the internet. Thanks to the use of a mobile power bank and PV

Table 2 General characteristics of the IOT system

Parameters	IoT system
Sensivity (LSB)	1.07 mV
Energy source	PV panel supported power bank
Input range	0 – 1.1 V
Op-amp gain	1:1
Working voltage	3.3 V
Current consumption	<30 mA idle, <100 mA average, <400 mA max.
Enclosure	3D printed with PLA
Sensor connector	2 mm banana plug cable with crocodile clip
Channel number	2 used, 16 total
Total cost	<$25

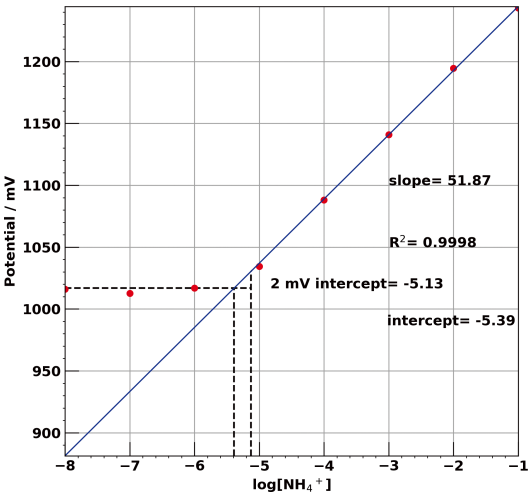


Fig. 5 Potentiometric response of the ammonium-selective ISE.

panel, portability and up-time problems related to energy needs were solved. We also measured current consumption data at 3.3 V with a multimeter, GDM-8341 (Gw Instek, Taiwan). The results are presented in Table 2, together with the summary characteristics of the system.

Potentiometric behavior of the electrodes

Potential response of the electrodes was measured using standard solutions of the relevant ions (10^{-1} to 10^{-8} mol L^{-1}), which were prepared by serial 10-fold dilutions of relevant 10^{-1} mol L^{-1} solutions. The results are shown in Figs. 5 and 6 and summarized in Table 3. Ammonium ISEs performed better than nitrate ISEs in terms of linear range, detection limit, and slope. These results were consistent with our previous studies.[31,32]

The ISEs we used in this paper showed a slight deviation from the ideal (59.16 mV/decade) value. This can be attributed to the membrane composition and the ratio of the materials used within. However, there are some studies in the literature with similar membrane structures, which showed a Nernstian response close to our ISEs.[12,33] Since our main purpose here is not to develop new ISEs but to exhibit how to incorporate the existing ISEs into a new wireless platform, the lack of ideal performance on the side of ISEs does not pose an issue.

The detection limit was determined from the intersection of the two extrapolated lines of the calibration curve (indicated as intercept in Figs. 5 and 6). The lower linear part of the curve

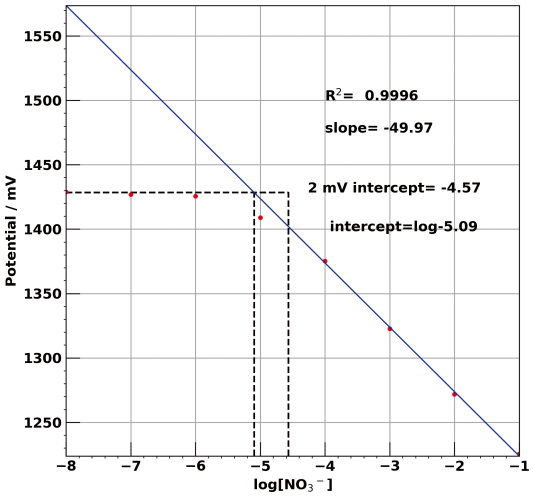


Fig. 6 Potentiometric response of the nitrate-selective ISE.

Table 3 Potentiometric characteristics of the ammonium and nitrate ISEs

	Linear range/ mol L^{-1}	Detection limit/ mol L^{-1}	R^2	Slope/ mV $decade^{-1}$
NO_3^- ISE	2.69×10^{-5} – 10^{-1}	8.13×10^{-6}	0.9996	–49.97
NH_4^+ ISE	7.41×10^{-6} – 10^{-1}	4.07×10^{-6}	0.9998	51.87

was determined as the point where the curve deviated 2 mV from linearity.[27]

Analytical application

To validate the usability of the electrodes the standard addition method was applied, and recovery rates were calculated. Tap water was used for recovery tests. While the ammonium ion level in the water was measured as $(2.72 \pm 1.09) \times 10^{-5}$ mol L^{-1}, the nitrate ion level was under the detection limit (8.13×10^{-6} mol L^{-1}). Ammonium chloride and calcium nitrate tetrahydrate were used to simulate ammonium and nitrate-contaminated tap water and to calculate recovery value. We first measured the levels of ammonium and nitrate ions in tap water. These values are shown as "detected" in Table 4. Then we added standards and measured again the artificially contaminated tap water. The latter values are presented as "found" in the table. Ammonium ISEs gave better results in recovery rates than nitrate ISEs. However, the recovery rates of the nitrate ISEs were very close to each other except for sample No. 1 (Table 4).

Interference of other ions

One of the reasons why the recovery values were not perfect is the interference effect of the other ions in the samples. Therefore, we determined the selectivity of the ISEs using the separate solution method ($a_A = a_B$) proposed by IUPAC.[34] The selectivity coefficient was calculated from Eq. (2):

$$\log K_{A,B}^{pot} = (E_B - E_A)/S + (1 - z_A/z_B) \log a_A \quad (2)$$

Here a_A and a_B are the activity of main ion A and interfering ion B, respectively. E_A and E_B are the measured potential values, and z_A and z_B are the charges of the ions A and B. S is the sensitivity of the A-selective electrode.[35] The selectivity of

Table 4 Recovery rates of ammonium and nitrate ISEs

Sample No	Ion	Detected[a]/mol L^{-1}	Added/mol L^{-1}	Found[a]/mol L^{-1}	Recovery, %
1	NO_3^-	nd[b]	1.61×10^{-4}	$(2.72 \pm 0.10) \times 10^{-4}$	147.01
	NH_4^+	$(2.72 \pm 1.09) \times 10^{-5}$	5.55×10^{-3}	$(5.68 \pm 0.17) \times 10^{-3}$	101.74
2	NO_3^-	nd	8.06×10^{-4}	$(9.47 \pm 1.05) \times 10^{-4}$	117.42
	NH_4^+	$(2.72 \pm 1.09) \times 10^{-5}$	5.55×10^{-3}	$(5.76 \pm 0.43) \times 10^{-3}$	103.15
3	NO_3^-	nd	1.61×10^{-3}	$(1.79 \pm 0.07) \times 10^{-3}$	111.27
	NH_4^+	$(2.72 \pm 1.09) \times 10^{-5}$	1.11×10^{-2}	$(1.16 \pm 0.04) \times 10^{-2}$	104.38
4	NO_3^-	nd	4.03×10^{-3}	$(4.77 \pm 0.41) \times 10^{-3}$	118.22
	NH_4^+	$(2.72 \pm 1.09) \times 10^{-5}$	1.11×10^{-2}	$(1.19 \pm 0.05) \times 10^{-2}$	106.80

a. In tap water (mean ± standard deviation, $n = 4$). b. Not detected.

Table 5 Selectivity coefficients (log $K_{A,B}^{pot}$) of the related ISEs

ISE	Selectivity coefficients		
NO_3^-	Cl^-: –2.63	SO_3^-: –2.24	CH_3COO^-: –2.03
NH_4^+	Na^+: –2.47	Ca^{2+}: –3.24	Ba^{2+}: –3.48
	K^+: –1.07	Mg^{2+}: –3.75	Sr^{2+}: –2.78

the electrodes was calculated against various common anions and cations given in Table 5. While potassium and sodium are the main interference ions for ammonium ISEs, acetate is the main interference ion for nitrate ISEs. Since the selectivity of the nitrate electrodes was not very high, the recovery rates were not close to 100%. Recovery rates can be closer to 100% if the samples were passed through an ion-exchange column prior to measurement.

Conclusions

This study can be considered as an immediate solution to the existing problems in preventing water pollution. Laboratory results clearly indicate that the IoT-enabled system we propose can work as intended to monitor water nitrate and ammonium levels. The presented system can also work with different ISEs to detect and measure various ions for future water quality monitoring applications. The primary output of this research is the remote access to analyses made with the IoT application, which is a modern version of the wireless connection providing 24/7 monitoring over the World Wide Web.

References

1. A. Mukherjee, A. K. Panja, and N. Dey, "*A Beginner's Guide to Data Agglomeration and Intelligent Sensing*", **2020**, Elsevier, 29.
2. J.-M. Dilhac and V. Boitier, "*Energy Autonomy of Batteryless and Wireless Embedded Systems*", **2016**, Elsevier, 1.
3. R. Taymanov and K. Sapozhnikova, "*Smart Sensors and MEMS: Intelligent Sensing Devices and Microsystems for Industrial Applications: Second Edition*", **2018**, Elsevier Inc., 1.
4. H. Qumber Ali and S. Ghani, *Comput. Networks*, **2020**, *181*, 107512.
5. K. Xu, Y. Kitazumi, K. Kano, and O. Shirai, *Anal. Sci.*, **2020**, *36*, 1141.
6. K. Nagamine, A. Nomura, I. Yusuke, I. Ryota, S. Sasaki, H. Furusawa, H. Matsui, and S. Tokito, *Anal. Sci.*, **2020**, *36*, 291.
7. P. Pang, X. Gao, X. Xiao, W. Yang, Q. Cai, and S. Yao, *Anal. Sci.*, **2007**, *23*, 463.
8. L. Schweitzer and J. Noblet, "*Green Chemistry: An Inclusive Approach*", **2018**, Elsevier Inc., 261.
9. M. A. P. Mahmud, F. Ejeian, S. Azadi, M. Myers, B. Pejcic, R. Abbassi, A. Razmjou, and M. Asadnia, *Chemosphere*, **2020**, *259*, 127492.
10. K. Lin, Y. Zhu, Y. Zhang, and H. Lin, *Trends Environ. Anal. Chem.*, **2019**, *24*, e00073.
11. H. Jeong, J. Park, and H. Kim, *J. Chem.*, **2013**.
12. J. Choosang, A. Numnuam, P. Thavarungkul, P. Kanatharana, T. Radu, S. Ullah, and A. Radu, *Sensors*, **2018**, *18*, 3555.
13. A. P. Murphy, *Nature*, **1991**, *350*, 223.
14. World Health Organization, "Guidelines for Drinking-Water Quality: Fourth Edition Incorporating the First Addendum", **2014**, World Health Organization.
15. J. Schullehner, L. Stayner, and B. Hansen, *Int. J. Environ. Res. Public Health*, **2017**, *14*, 276.
16. J. Mertens, P. Van den Winkel, and D. L. Massart, *Anal. Chem.*, **1975**, *47*, 522.
17. M. Pule, A. Yahya, and J. Chuma, *J. Appl. Res. Technol.*, **2017**, *15*, 562.
18. P. Kassal, M. D. Steinberg, and I. M. Steinberg, *Sens. Actuators, B*, **2018**, *266*, 228.
19. B. W. Abegaz, T. Datta, and S. M. Mahajan, *Appl. Energy*, **2018**, *210*, 451.
20. L. Nuñez, X. Cetó, M. I. Pividori, M. V. B. Zanoni, and M. del Valle, *Microchem. J.*, **2013**, *110*, 273.
21. L. Wang, Y. Cheng, D. Lamb, M. Megharaj, and R. Naidu, *Environ. Technol. Innov.*, **2019**, *15*, 100424.
22. V. Belikova, V. Panchuk, E. Legin, A. Melenteva, D. Kirsanov, and A. Legin, *Sens. Actuators, B*, **2019**, *282*, 854.
23. J. V. V. Capella, A. Bonastre, R. Ors, and M. Peris, *Talanta*, **2010**, *80*, 1789.
24. M. R. Gartia, B. Braunschweig, T. W. Chang, P. Moinzadeh, B. S. Minsker, G. Agha, A. Wieckowski, L. L. Keefer, and G. L. Liu, *J. Environ. Monit.*, **2012**, *14*, 3068.
25. J. V. Capella, A. Bonastre, R. Ors, and M. Peris, *Sens. Actuators, B*, **2013**, *177*, 419.
26. E. E. Totu, I. Isildak, O. Tavukcuoglu, I. Agir, R. Yildirim, M. Nigde, A. C. Nechifor, and C. M. Cristache, *Rev. Chim.*, **2018**, *69*, 3213.
27. R. Yildirim, I. Agir, M. Nigde, and I. Isildak, *Int. J. Electrochem. Sci.*, **2020**, *15*, 11468.
28. R. K. Franklin, S. M. Martin, T. D. Strong, and R. B. Brown, "*Reference Module in Materials Science and Materials Engineering*", **2016**, Elsevier.

29. LMP7721 data sheet, product information and support | TI.com, https://www.ti.com/product/LMP7721#tech-docs.
30. S. J. Tilden, S. Max, J. Blair, F. Alegria, E. Balestrieri, N. Bjorsell, J. Calvin, D. Dallet, P. Daponte, L. De Vito, A. Goncharenko, D. Greer, R. Liggiero, T. E. Linnenbrink, S. Rapuano, and F. Xu, "*IEEE Std.1241-2010-IEEE Standard for Terminology and Test Methods for Analog-to-Digital Converters (Revision of IEEE Std.1241-2000)*", **2011**.
31. G. Vardar, M. Altikatoğlu, D. Ortaç, M. Cemek, and I. Işildak, *Biotechnol. Appl. Biochem.*, **2015**, *62*, 663.
32. M. Altikatoglu, E. Karakus, V. Erci, S. Pekyardımcı, and I. Isildak, *Artif. Cells, Nanomed., Biotechnol.*, **2013**, *41*, 131.
33. J. Schwarz, K. Trommer, and M. Mertig, *Am. J. Anal. Chem.*, **2018**, *9*, 591.
34. Y. Umezawa, P. Bühlmann, K. Umezawa, K. Tohda, and S. Amemiya, *Pure Appl. Chem.*, **2000**, *72*, 1851.
35. T. Ozer and I. Isildak, *Int. J. Electrochem. Sci.*, **2018**, *13*, 11375.